Available online at www.sciencedirect.com
SCIENCE DIRECT®
Atmospheric Environment 39 (2005) 5291–5306
ATMOSPHERIC ENVIRONMENT
www.elsevier.com/locate/atmosenv

Simulated sensitivity of seasonal ozone exposure in the Great Lakes region to changes in anthropogenic emissions in the presence of interannual variability

Jerome D. Fast[a,*], Warren E. Heilman[b]

[a]*Pacific Northwest National Laboratory, Richland, WA 99352, USA*
[b]*USDA Forest Service, East Lansing, MI, USA*

Received 9 February 2005; accepted 13 May 2005

Abstract

A coupled meteorological and chemical modeling system with a 12-km horizontal grid spacing was used to simulate the evolution of ozone over the Great Lakes region between May and September of 1999 and 2001. The overall temporal and spatial variations in hourly ozone concentrations and ozone exposure from control simulations agreed reasonably well with the observations at most locations with an overall monthly bias computed across all stations ranging from −3.2 to 5.3 ppb, the root mean square difference ranging from 18.2 to 22.2 ppb, and an index of agreement ranging from 0.63 to 0.78. As with the observations, the simulated ozone exposure was higher during most months of the summer of 1999 than during 2001. Sensitivity simulations that increased anthropogenic trace gas emissions were performed to determine the changes in ozone exposure in the presence of meteorological interannual variability. The emission scenario simulations that employed the meteorological conditions of 1999 and increased anthropogenic emissions of NO*x* and VOCs produced increases in ozone exceeding 80 ppb over the lower peninsula of Michigan, the eastern half of the upper peninsula of Michigan, and over Ontario just north of Lake Superior and Lake Huron. Over the agricultural regions, more ozone between 60 and 80 ppb was produced. The cooler and wetter conditions with more frequent periods of northwesterly flow during the summer of 2001 were not as favorable for ozone production and did not result in increased ozone, despite the increase in anthropogenic emissions. Increases in ozone exceeding 60 ppb occurred only over the lake surfaces and in central Michigan when the meteorological conditions of the summer of 2001 were applied. For both summers, increases in anthropogenic emissions decreased ozone exposure in the immediate vicinity of the largest metropolitan areas. Since anthropogenic emission rate projections depend on assumptions of population, economic development, land-use patterns, and technology, the effect of anthropogenic emission rates on the magnitude and regional-scale distribution of ozone concentrations could be much larger or smaller than indicated by this study. In a subsequent study, the simulated ozone will be used as input to biological models to assess the response of ozone-sensitive tree species in the Great Lakes region to ozone levels produced by various anthropogenic emission scenarios.

Keywords: Regional photochemical modeling; Air quality; Ozone exposure; Boundary layer; NO*x*; VOC

*Corresponding author.
E-mail address: jerome.fast@pnl.gov (J.D. Fast).

1352-2310/$ - see front matter © 2005 Published by Elsevier Ltd.
doi:10.1016/j.atmosenv.2005.05.032

1. Introduction

In addition to the effects of ozone on human health, high surface ozone concentrations can have an adverse effect on specific types of vegetation (McKee, 1994). Global and regional-scale climate model predictions indicate human activities will likely alter the average meteorological conditions over the next several decades (IPCC, 2001). Possible changes in synoptic and mesoscale weather patterns as well as local wind speed, temperature, humidity, boundary layer depth, cloudiness, and precipitation will affect the production/destruction, turbulent mixing, transport, and deposition of ozone.

Future vegetation health will depend also on interactions between meteorological parameters and pollutant emission rates that influence the distribution and concentration of ozone. In addition to greenhouse gases (e.g. carbon dioxide), anthropogenic emissions of ozone precursors such as nitrogen oxides and hydrocarbons are estimated to increase during this century (IPCC, 2000). Other studies, however, have indicated declines in anthropogenic emissions over the past five to 10 years (US EPA, 2004). Climate change and human activities can directly and indirectly affect biogenic emissions by altering surface temperature and vegetation distributions (Constable et al., 1999; Civerolo et al., 2000). Modeling studies also suggest that the impact of long-range transport on local air quality will increase in the future (Jacob et al., 1999; Yienger et al., 2000).

Despite the number of global climate simulations, only a few have examined the impact of climate change on tropospheric chemistry (Brasseur et al., 1998; Fiore et al., 2002; Johnson et al, 1999; Prather et al., 2003). Higher resolution simulations are needed to assess the impacts of climate change on human and vegetation health because global models do not resolve the large variations in anthropogenic trace gas emissions associated with urban and point sources. Urban to regional-scale models have been applied to simulate air pollution episodes lasting from a few days to weeks, but they are now being applied to assess the interaction between climate and regional air quality. For example, Hogrefe et al. (2004) recently completed a series of simulations for the eastern US using a 36-km model grid spacing to predict ozone levels for the summers of 2020, 2050, and 2080. They found that ozone predictions in the eastern US were most sensitive to changes in large-scale chemical environment that alter the regional trace gas boundary conditions. Regional climate change and increased anthropogenic emissions had a smaller impact on ozone than the large-scale chemical environment, except during high ozone events when regional climate change became the dominant factor.

The objectives of this study are to (1) determine the effect of changes in anthropogenic trace gas emissions on local and regional variations of ozone exposure in the Great Lakes Region and (2) develop a set of current and future regional ozone exposure scenarios that can be used as input to vegetation response models for assessing ozone risk to forest health. A coupled meteorological and chemical modeling system is used to simulate the evolution of ozone during the summers of 1999 and 2001 with contrasting meteorological conditions. The warmer and drier synoptic conditions over much of the eastern US during the summer of 1999 were favorable for ozone production, while cooler and wetter conditions with more frequent periods of northwesterly flow during the summer of 2001 reduced ozone concentrations. Additional simulations were performed to examine the effect of increased anthropogenic trace gas emission rates on ozone exposure and how sensitive the predicted changes in ozone concentrations are to the different meteorological conditions between these two summer seasons. In a future study, the simulated current and future ozone exposure distributions will be employed to assess the impact of increased anthropogenic emissions on forest health in the Great Lakes region.

2. Simulation period

The Pacific Northwest National Laboratory (PNNL) Eulerian Gas and Aerosol Unified System (PEGASUS), as described by Fast et al. (2002), was used to simulate the evolution of ozone for a five-month period between 1 May and 30 September for 1999 and 2001. These two summers were examined because of the different overall meteorological conditions that resulted in a variety of seasonal and monthly ozone patterns in the region.

Ozone exposure is a useful quantity to assess the potential impact of ozone on vegetation health (Hogsett et al., 1997). We employ the SUM60 and SUM80 biological indices defined as:

$$\text{SUM60 (ppb h)} = \sum [O_3]\Delta t, \quad \text{for } [O_3] > 60\text{ppb}, \tag{1}$$

$$\text{SUM80 (ppb h)} = \sum [O_3]\Delta t, \quad \text{for } [O_3] > 80\text{ppb}. \tag{2}$$

While certain types of vegetation become damaged during long-term exposure to ozone greater than 60 ppb (Hogsett et al., 1997), exposure to ozone greater than 80 ppb also is computed to determine the frequency of higher ozone levels associated with air pollution episodes. The observed monthly ozone exposure for all ozone monitors in the Great Lakes region (see Fig. 1) is shown in Fig. 2. Ozone measurements were obtained from the US EPA's operational network, including the clean air status and trends network (CASTNET), and Environment Canada's National Air Pollution Surveillance (NAPS) network. The mean and range of SUM60 and SUM80 were higher during 1999 than 2001 for the

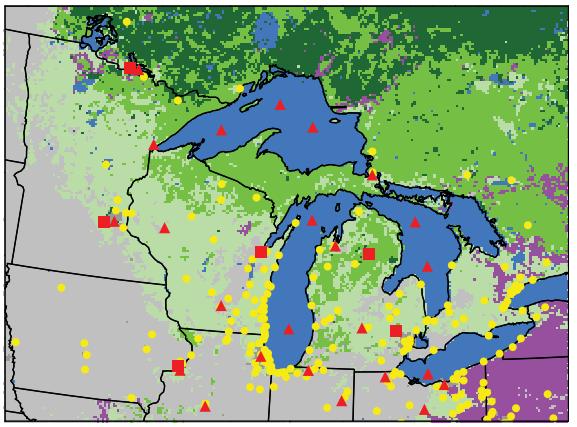

Fig. 1. Dominant vegetation types over the second modeling domain: crop and mixed farming (light gray), wooded grassland (light green), mixed woodland (green), evergreen needleleaf forest (dark green), and deciduous broadleaf forest (purple). Operational ozone monitoring stations denoted by yellow circles and meteorological surface and upper-air stations denoted by red triangles and squares, respectively.

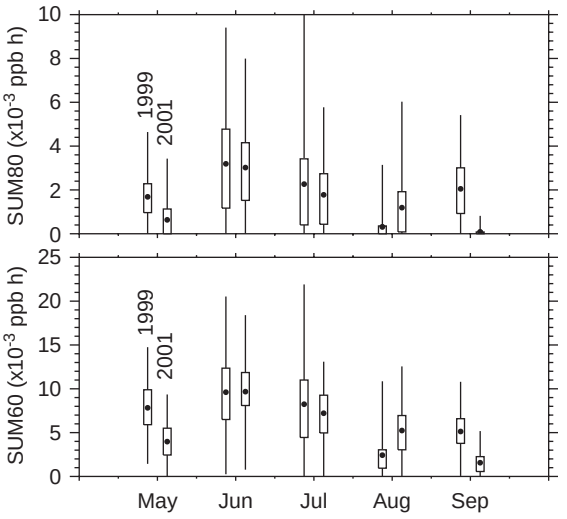

Fig. 2. Observed SUM60 and SUM80 over the Great Lakes region during the summer of 1999 and 2001. The vertical lines denote the range, the boxes denote the 25% and 75% quantiles, and the dots the average among the monitoring stations shown in Fig. 1. The median values are close to the average values (not shown).

months of May, July, and September. Ozone exposures during June of 1999 and 2001 were similar and August was the only month in which exposure was higher in 2001 than in 1999.

To illustrate that the differences in ozone levels were related to the meteorological patterns, monthly averaged 850-h Pa geopotential heights and winds based on the National Center for Environmental Prediction's (NCEP) AVN model 00 UTC and 12 UTC analyses are shown in Fig. 3 along with the 20-year mean for May. The climatological mean field (Fig. 3a) has a high-pressure system over the southeastern US and westerly flow over the Great Lakes region. These synoptic meteorological conditions have been shown (Vukovich, 1987, 1995) to be favorable for ozone formation in the eastern US. The 20-year means for the other months were similar to May, except for slight differences in the center of the high-pressure system.

During May of 1999 the ridge of high pressure was centered over the Appalachian Mountains, while the ridge extended into eastern Canada with a trough of low pressure just west of the Great Lakes during May of 2001 (Fig. 3b). The synoptic conditions during both May of 1999 and 2001 produced mean southwesterly flow over the Great Lakes; however, the trough west of the Great Lakes during May of 2001 indicates that more cold fronts passed through the region that transported polluted air to the east and reduced ozone exposure when compared to May of 1999 (Fig. 2). The mean synoptic patterns during June of 1999 and 2001 (Fig. 3c) were nearly identical, consistent with the observed ozone exposure that also was similar for those two years. While the synoptic flow pattern during July 1999 was similar to the 20-year mean, northwesterly flow over the eastern US frequently occurred during 2001 (Fig. 3d). The northwesterly flow transported air with lower ozone concentrations from Canada into the Great Lake region, producing lower ozone exposure during 2001 than 1999. The situation reversed in August (Fig. 3e) so that more northwesterly flow and lower ozone exposures occurred during 1999. During September of 2001, the mean synoptic conditions departed significantly from the 20-year mean conditions with frequent periods of northerly flow that resulted in few air pollution episodes with ozone exceeding 80 ppb in the Great Lakes region (Fig. 3f). The synoptic conditions of westerly flow during 1999 were still favorable for ozone production.

As will be discussed later, the variations in the meteorological conditions and the contrasting synoptic conditions between 1999 and 2001 were useful in illustrating the potential impact of emission scenarios on ozone concentrations in the region.

3. Model description

3.1. Domain

Two nested grids were employed by PEGASUS: an outer domain that included most of eastern North America with a grid spacing of 36 km and an inner domain as shown in Fig. 1 that encompassed the western

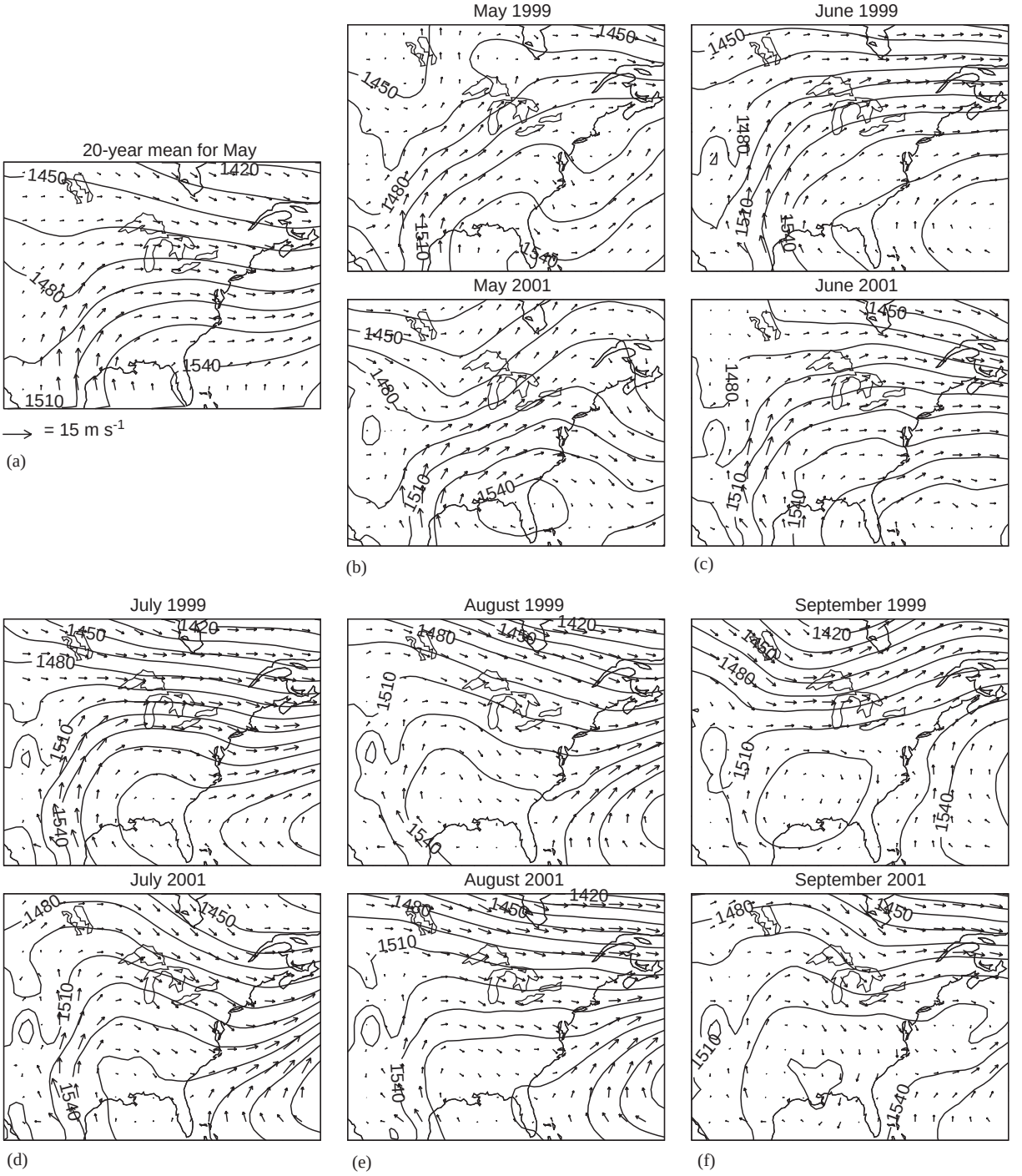

Fig. 3. The monthly mean 850-h Pa geopotential heights and winds including the (a) 20-year mean for May between 1980 and 2000 and the means for (b) May, (c) June, (d) July), (e) August, and (f) September for 1999 and 2001.

Great Lakes region with a grid spacing of 12 km. Fifty grid points were used for the vertical coordinate, with a grid spacing of 25 m adjacent to the surface that gradually increased to 750 m near the model top at 20 km. Due to the staggered vertical coordinate, the first grid point was 12.5 m AGL.

3.2. Initial and boundary conditions

The initial and lateral boundary conditions for the meteorological simulations were based on the NCEP AVN model analyses at 6-h intervals. To limit forecast errors in the synoptic conditions over the five-month simulation period, four-dimensional data assimilation was applied that nudged the simulated winds, temperature, and humidity towards the AVN model analyses (Fast, 1995). Lake temperatures on the inner nested grid varied linearly in time based on the NOAA Great Lakes Environmental Research Laboratory daily 3-km analyses derived from satellite data (Schwab et al., 1992).

Hourly fields of the horizontal and vertical winds, temperature, humidity, eddy diffusivity, cloud parameters, and surface properties from the mesoscale model were used to drive the chemical transport model. The chemical transport model employs the same eddy exchange coefficients determined from the mesoscale model's predicted turbulence kinetic energy (Mellor and Yamada, 1982; Helfand and Labraga, 1988) so that treatment of vertical mixing is consistent in both models. Cumulus and microphysics parameterizations in the mesoscale model were employed to predict clouds and precipitation on both grids and the predicted cloud parameters influenced photolysis rates and large-scale vertical mixing of trace gases.

The initial and boundary conditions for ozone on the outer grid in the upper troposphere and lower stratosphere were based on predicted potential vorticity (Danielsen et al., 1987) to represent large-scale stratosphere–troposphere exchange processes. Ozone in the lower troposphere was set to 30 ppb and the values in middle troposphere varied linearly between 30 ppb and the values obtained in the upper troposphere. Initial and boundary conditions for the other trace gas species on the outer grid were set to constant background values as in Fast et al. (2002). The chemical transport model employs one-way nesting so that ozone and ozone precursors produced over the outer grid were used as time varying boundary conditions on the inner grid.

3.3. Emission rates

Hourly emission rates of 15 trace gases over the US and southern Canada were obtained from the Sparse Matrix Operator Kernel Emissions (SMOKE) model (Houyoux et al., 2000) and based on the 1995 ozone transport assessment group (OTAG) inventory. The SMOKE emission rates and plume rise were generated off-line over the eastern US and southern Canada on a 4-km grid using the simulated meteorological conditions from the outer domain of the mesoscale model. The emission rates were then aggregated to the 36 and 12-km grid cells used by the two domains. The highest emission rates occurred over urban areas; however, a few point sources with high emission rates were located along the shores of Lake Superior and Lake Huron. Over northern Canada, emission rates were obtained from the EDGAR global inventory (Olivier and Berdowski, 2001). A parameterization described by Guenther et al. (1993) and the predicted meteorological conditions from both domains were used to generate isoprene emission rates.

3.4. Types of simulations

Two sets of simulations were performed: "control simulations" and "emission scenario simulations". The control simulations were designed to reproduce, as best as possible, the evolution of the observed spatial distribution and magnitude of ozone in the Great Lakes region throughout the 1999 and 2001 summer seasons. Predicted ozone exposure was evaluated with the available observations (Fig. 1). As will be shown later, the simulated diurnal and multi-day variations in ozone as well as the monthly and seasonal ozone exposure were usually consistent with the available measurements. Most of the ozone monitors are located in the vicinity of urban areas (Fig. 1); however, a number of monitors are located in the remote forested regions surrounding the Great Lakes.

The emission scenario simulations were identical to the control simulations, except that the NOx and VOC anthropogenic emission rates were increased by a constant factor over the entire domain for both surface and point sources. NOx and VOC emission rates were increased by a factor of 1.25 and 1.08, respectively, for emission scenario 'A' and by a factor of 1.35 and 1.25, respectively, for emission scenario 'B'. Emission scenarios 'A' and 'B' were based on the overall estimated emission increases in developed countries for 2020 and 2040, respectively, as described in the Intergovernmental Panel on Climate Change (IPCC) Special Report on Emissions Scenarios (SRES) B2 marker scenario (IPCC, 2000). The IPCC estimates do not account for local and regional variations in emission changes as well. Projections of anthropogenic trace gas emissions have large uncertainties that depend on assumptions of population, economic development, land-use patterns, and technology. In fact, US EPA (2004) report recent declines in NOx and VOC emission rates of ~17% between 1997 and 2002 and the emission rates for 2020 that were lower than the 1996 National Emission Trends database in the modeling study of Tao et al. (2003) because of the assumed adherence to strict state implementation plans. Therefore, the ozone predictions from emission scenario simulations 'A' and 'B' result from hypothetical, but plausible, increases in ozone precursors.

4. Results

We first present a comparison of the observed and simulated meteorology and ozone during the summers of 1999 and 2001 from the control simulations. Then, the effects of higher anthropogenic emission rates estimated for emission scenarios 'A' and 'B' on ozone exposure in the Great Lakes region are quantified.

4.1. Meteorological evaluation

The simulated winds, temperatures, and humidity from the mesoscale model have been compared with hourly surface meteorological stations and twice-daily upper air soundings at 00 at 12 UTC. The simulated winds followed the observed synoptic patterns during the five-month period (not shown) as expected because the model employed four-dimensional data assimilation.

An example of the observed and simulated wind speed, direction, and temperature at Lansing Michigan for July 1999 is shown in Fig. 4. The model reproduced the magnitude and multi-day variation of maximum surface temperature well, but the diurnal temperature range was too low. The simulated nighttime minimum temperatures were 1 °C–3 °C too high. Since the first grid point was 12.5 m AGL and the observations were at 2 m AGL, stratification within the nocturnal boundary layer would account for part of the differences between the observed and simulated nighttime temperatures. The predicted wind speeds and directions were similar to the observations with a correlation coefficient of 0.74 and 0.65, respectively.

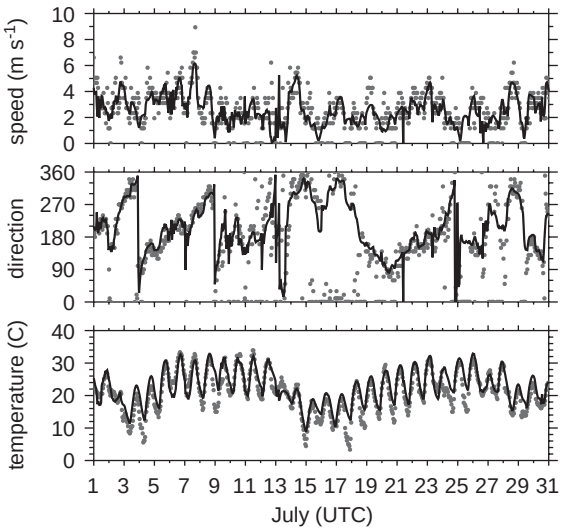

Fig. 4. Time series of observed (dots) and predicted (line) near-surface wind speed, direction, and temperature at Lansing, Michigan for July 1999.

Statistics that quantify the performance of the simulated surface temperature, wind speed, and direction are given in Table 1 for the stations shown in Fig. 1. Performance statistics include the bias, the root-mean-square difference, RMSD, and the index of agreement, IA, defined by

$$\text{bias} = \frac{1}{N}\sum_{i=1}^{N} p_i - o_i, \tag{3}$$

$$\text{RMSD} = \left[\frac{1}{N}\sum_{i=1}^{N}(p_i - o_i)^2\right]^{1/2}, \tag{4}$$

$$\text{IA} = \frac{\sum_{i-1}^{N}(p_i - o_i)^2}{\sum_{i-1}^{N}(|p_i - \bar{o}| + |o_i - \bar{o}|)^2}, \tag{5}$$

where p_i and o_i are the simulated and observed values, N is the total number of hourly measurements, and the overbar denotes a monthly average. An index of agreement of 1 indicates perfect agreement between the observed and predicted variables and 0 indicates no agreement at all (Willmott, 1982). The standard deviation of bias, RMSD, and IA also are included in Table 1 to describe the variation of the performance statistics among the measurement locations.

The monthly index of agreement was greater than 0.87, 0.72, 0.67, and 0.76 for temperature, relative humidity, speed, and direction, respectively, indicating that the mesoscale model produced much of the observed variations during the five-month period. Most of the positive bias in temperature results resulted from higher than observed predicted nighttime temperatures, as shown in Fig. 4. The warm bias also contributed to the negative bias in predicted relative humidity. While there was little bias in the wind speed, wind directions differed from the observations by 7°–14° on average.

The winds aloft were evaluated by comparing the simulated results with the 00 and 12 UTC rawinsonde winds that were not directly employed by data assimilation in PEGASUS but were indirectly employed through the AVN analyses. Time series of wind speed, direction, temperature, and relative humidity at the rawinsonde sites showed that the model predicted well the observed trends in temperature, humidity, speed, and direction throughout the five-month period (not shown).

The bias in the wind speed, direction, temperature, and relative humidity within 3.5 km of the ground for the Alpena, Michigan rawinsonde during the summer of 1999 are shown in Fig. 5. On average, the model winds were slightly lower than observed, except near the surface where the simulated wind speed was 1.8 m s^{-1} too low, consistent with the comparison with the surface observations (Fig. 4). The bias in the wind directions was usually less than 5°. Some of the wind direction errors were associated with timing errors in the

Table 1
Performance statistics for predicted surface meteorology using the stations denoted in Fig. 1

Statistic	May	Jun.	Jul.	Aug.	Sept.
Temperature: average IA	0.93	0.92	0.89	0.87	0.94
Temperature: σ_{AI}	0.04	0.05	0.07	0.07	0.04
Temperature: average RMSD	3.3	3.3	3.4	3.0	3.1
Temperature: σ_{RMSD}	0.52	0.47	0.63	0.60	0.53
Temperature: Average bias	2.3	1.5	1.4	1.4	1.2
Temperature: σ_{bias}	0.58	0.72	1.05	0.85	0.60
Relative humidity: Average IA	0.85	0.84	0.78	0.72	0.80
Relative humidity: σ_{AI}	0.10	0.13	0.17	0.16	0.14
Relative humidity: Average RMSD	18.7	18.6	21.2	20.8	19.4
Relative humidity: σ_{RMSD}	2.9	3.0	5.1	4.8	2.7
Relative humidity: Average bias	−13.2	−12.1	−15.0	−15.4	−13.3
Relative humidity: σ_{bias}	3.7	4.0	5.7	5.7	3.3
Wind speed: Average IA	0.81	0.66	0.69	0.67	0.71
Wind speed: σ_{AI}	0.05	0.14	0.17	0.24	0.17
Wind speed: Average RMSD	12	1.4	1.4	1.6	1.2
Wind speed: σ_{RMSD}	0.20	0.58	0.50	1.26	0.54
Wind speed: Average bias	0.1	−0.1	−0.1	−0.1	0.1
Wind speed: σ_{bias}	0.35	0.25	0.27	0.33	0.31
Wind direction: Average IA	0.86	0.76	0.79	0.79	0.76
Wind direction: σ_{AI}	0.06	0.07	0.05	0.05	0.05
Wind direction: Average RMSD	62.5	82.4	68.9	93.9	84.0
Wind direction: σ_{RMSD}	17.0	17.0	15.5	11.3	14.2
Wind direction: Average bias	2.0	7.9	8.2	7.0	3.4
Wind direction: σ_{bias}	6.9	11.3	11.6	11.3	14.2

The statistics in Table 1 are first computed for individual stations and then averaged among all the sites.

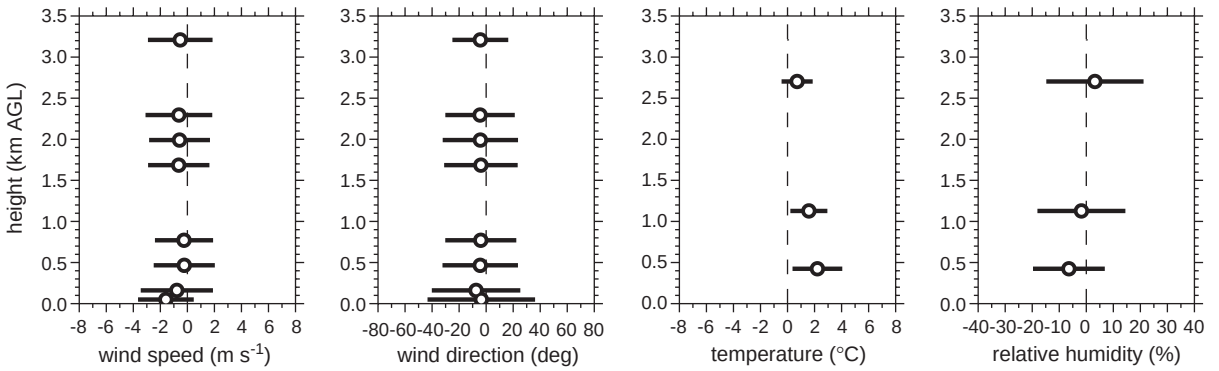

Fig. 5. Bias (circles) and standard deviation (lines) of wind speed, direction, temperature, and relative humidity at Alpena, Michigan between May and September 1999.

propagation of synoptic systems, such as the passage of a cold front, of a few hours or less. At elevations usually within the afternoon convective boundary layer, temperatures were ~2 °C too warm and relative humidity was too low by 7% In the free troposphere, the mean temperature and relative humidity biases were close to zero. The overall errors for the other rawinsonde stations for 1999 and 2001 were similar to those shown in Fig. 5.

Cloudiness and precipitation are the parameters with the largest uncertainty in mesoscale models. A qualitative agreement was found between the simulated spatial cloud distribution and satellite images of the observed cloud distribution (not shown), especially when fronts were moving through the region. However, the amount of cloudiness was significantly different than observed on some days and at specific locations as expected.

4.2. Ozone evaluation

Since the mesoscale model reproduced the main features of the observed winds and boundary layer evolution, the chemical transport model is expected to provide a reasonable estimate of regional-scale production and transport of pollutants during the two five-month periods. The near-surface warm bias, however, may lead to an over-estimate in the biogenic ozone precursor emission rates on some days. An example of the observed and predicted spatial variations in ozone is shown in Fig. 6 for a high ozone episode on 23 June 1999.

Ozone mixing ratios exceeded 80 ppb in the morning at 16 UTC over much of Michigan (Fig. 6a) as a result of ozone produced the previous day that remained aloft during the night and was entrained into the convective boundary layer (not shown). Ozone mixing ratios increased to 90–100 ppb during the afternoon by 20 UTC over many parts of Michigan, Indiana, Ohio and southern Ontario (Fig. 6b). Higher ozone mixing ratios between 110 and 120 ppb were present over parts of the lakes during the afternoon because the shallow stable boundary layer limited the vertical mixing of ozone and ozone precursors (Fast and Heilman, 2003). The higher ozone concentrations over the lake surfaces were

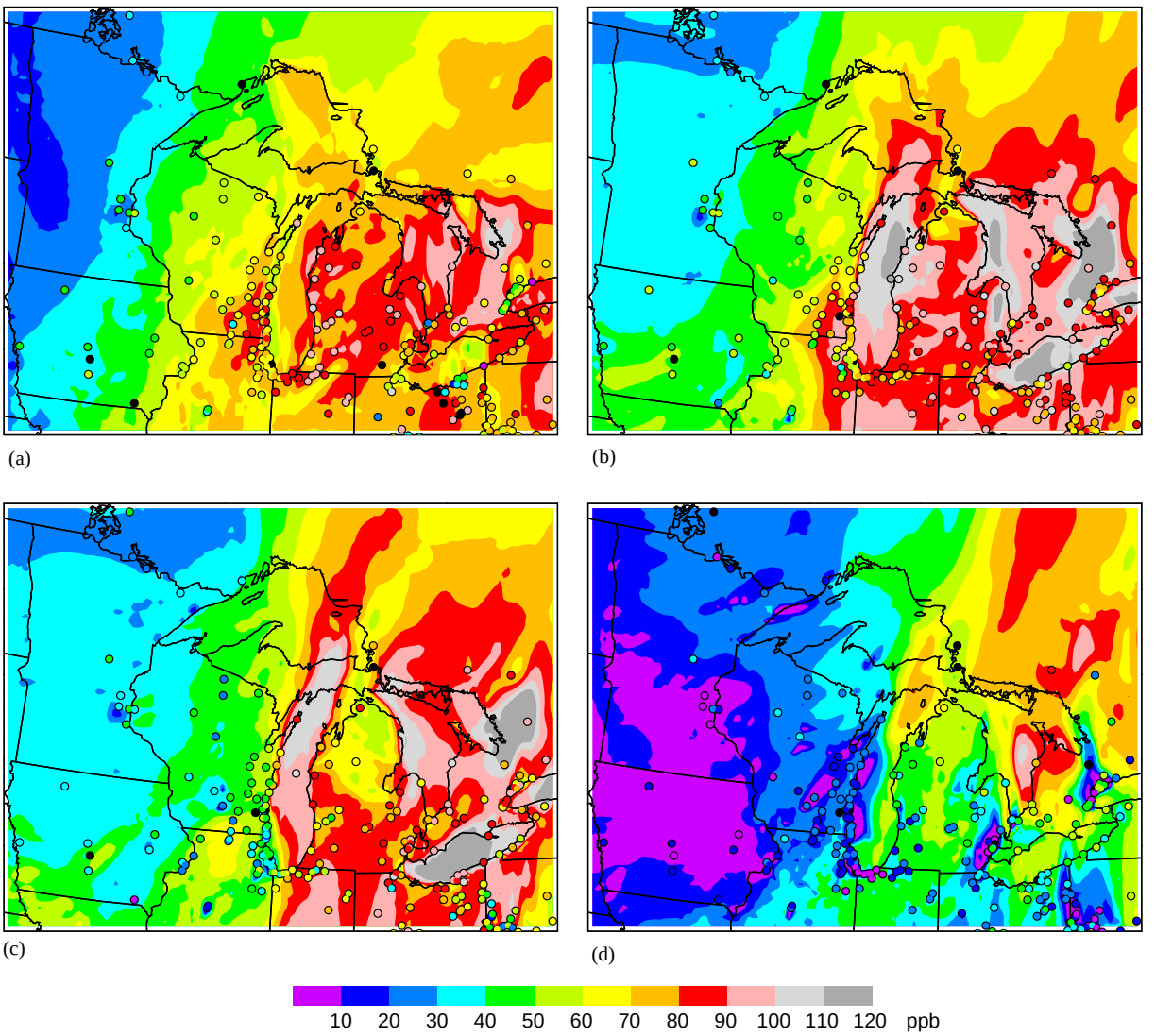

Fig. 6. Observed (circles) and predicted (contours) surface ozone during a typical high ozone episode at (a) 16 UTC 23 June, (b) 20 UTC 23 June, (c) 00 UTC 24 June, and (d) 10 UTC 24 June 1999.

consistent with measurements made on a ferry that crossed central Lake Michigan several times a day (Fig. 6b and c). Southerly winds transported ozone produced by anthropogenic emissions in the southern Great Lakes into the forested regions of the upper peninsula of Michigan and Ontario (Fig. 6c) just before sunset (00 UTC. Southerly flow continued to transport the ozone plumes into Canada during the night (Fig. 6d). While ozone mixing ratios decreased to less than 40 ppb in the vicinity of the highest precursor emission rates, ozone mixing ratios were still high during the evening at 10 UTC over northern Michigan and Ontario.

Time series of predicted ozone over the summer periods were compared with the available surface monitoring data. An example of the observed and predicted ozone at five sites is shown in Fig. 7 for June of 1999. The model qualitatively reproduced the diurnal and multi-day variation in ozone at northern sites (A and B) and southern sites (D and E) located far from and close to areas of high anthropogenic emission rates, respectively. For the southern sites, the observed and simulated ozone shows strong diurnal variation with afternoon ozone mixing ratios often exceeding 80 ppb and nighttime mixing ratios dropping to near zero as a result of nitrogen oxide titration. At the northern sites, the observed and simulated diurnal variation in ozone was much less. Afternoon peak values were lower because dispersion lowered the concentrations as pollutant plumes were transported northward and the lower anthropogenic emission rates would lead to lower local ozone production. At night, the lower anthropogenic emissions also would reduce the amount of nitrogen oxide titration. Observed and simulated ozone concentrations over central Lake Michigan at site C, were higher than those over land (such as site D) on many days because of the shallow boundary layer that reduced vertical mixing and enhanced photochemical production.

There are days in which PEGASUS, as with all air quality models, over- or under-predicted the afternoon peak ozone mixing ratios. The observed ozone mixing ratios, however, usually fall within the range of predicted ozone within three grid cells around the observation location, as indicated by the gray shading in Fig. 7. The range of surrounding predicted ozone is useful to examine because a small error in the wind speed can lead to transport errors equivalent to a few grid cells over several hours. The differences between the observed and simulated ozone for the other months and for other stations are similar to those in Fig. 7.

Statistics summarizing the model performance are listed in Table 2. The statistics are based on hourly values that evaluate both daytime and nighttime performance and employ data with nearly complete records from 161 and 34 stations in the United States and Canada, respectively. The monthly ozone mixing

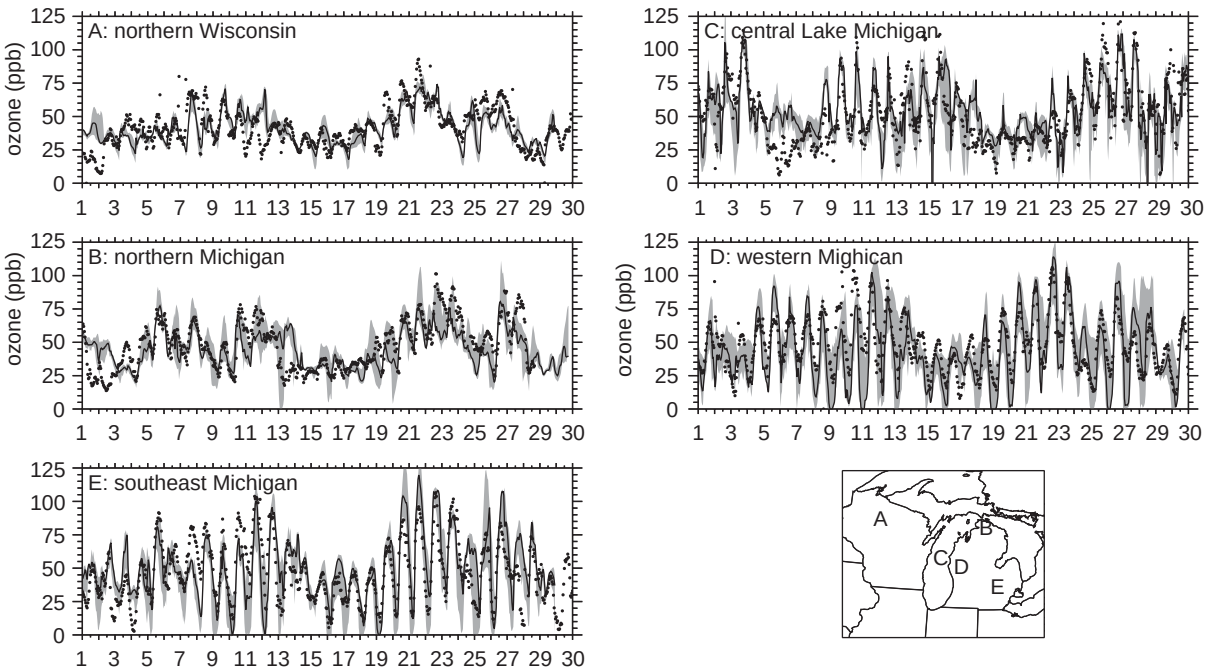

Fig. 7. Observed (dots) and predicted (line) ozone at 5 sites during June 1999. Gray shading denotes predicted values within 36 km of the monitoring sites.

Table 2
Performance statistics for predicted ozone over the inner nested grid (Fig. 1) using 161 ozone monitoring stations with at least two weeks of hourly data available per month

Period	Average IA	Standard deviation of IA	Average RMSD	Standard deviation of RMSD	Average bias	Standard deviation of bias
May 1999	0.73	0.06	18.3	3.2	−2.2	5.8
June 1999	0.75	0.06	20.4	4.7	−0.4	7.1
July 1999	0.74	0.06	19.6	4.7	−2.3	7.2
August 1999	0.69	0.07	18.9	3.9	2.7	7.4
September 1999	0.78	0.07	19.1	3.6	1.3	7.7
May 2001	0.63	0.08	18.4	3.4	−3.2	9.3
June 2001	0.72	0.06	22.2	4.2	1.2	7.5
July 2001	0.71	0.07	20.8	4.7	−1.0	8.2
August 2001	0.72	0.06	20.9	4.2	5.2	7.7
September 2001	0.68	0.07	18.1	3.2	5.3	7.5
Summer 1999	0.74	0.06	19.3	4.0	−0.9	7.0
Summer 2001	0.69	0.07	20.1	3.9	1.5	8.0

Table 3
Same as Table 2, except for daily maximum ozone

Period	Average IA	Standard deviation of IA	Average RMSD	Standard deviation of RMSD	Average bias	Standard deviation of bias
May 1999	0.75	0.08	15.5	3.2	−0.7	6.5
June 1999	0.76	0.09	16.2	4.7	1.4	8.3
July 1999	0.65	0.11	16.7	4.6	1.8	8.5
August 1999	0.62	0.13	16.2	4.6	6.5	8.5
September 1999	0.83	0.09	15.7	4.1	2.9	8.0
May 2001	0.59	0.10	15.5	3.4	−1.5	6.7
June 2001	0.70	0.11	19.7	4.5	5.9	7.4
July 2001	0.68	0.13	17.7	5.5	3.2	8.0
August 2001	0.66	0.10	19.7	5.5	11.4	7.6
September 2001	0.74	0.09	14.9	3.7	7.3	7.5
Summer 1999	0.72	0.10	16.1	4.2	2.4	8.0
Summer 2001	0.67	0.11	17.5	4.5	5.3	7.4

ratio bias ranged from −3.2 to 5.3 ppb and the monthly RMSD ranged from 18.1 to 22.2 ppb. The bias over the summer season was −0.9 ppb during 1999, and the bias of 1.5 ppb for 2001 was produced primarily from over-predictions in ozone during August and September. The agreement between the observed and simulated ozone is moderate with the monthly values of IA between 0.63 and 0.78.

Because ozone exposure greater than 60 or 80 ppb usually occurs during the daytime, similar statistics for the daily maximum ozone mixing ratio are listed in Table 3. These statistics indicate a slight under-prediction of the peak ozone during May, but the predicted peak ozone was too high by 1.4–11.4 ppb on average during the rest of the months. The monthly IA for the daily maximum ozone was similar to the monthly values determined from hourly values.

4.3. Ozone exposure

The SUM60 and SUM80 ozone exposure indices computed between May and September for each year are shown in Fig. 8. PEGASUS reproduced the overall spatial distribution and magnitude of ozone exposure. During 1999, the highest observed and predicted 80-ppb ozone exposure usually occurred at monitoring stations located along the eastern shore of Lake Michigan and south of Lake Erie. The model produced the highest ozone exposures over the lake surfaces because of the frequent shallow stable boundary layers and the proximity of urban precursors sources, such as Chicago, Milwaukee, and Cleveland. The observed and simulated SUM60 and SUM80 distributions were similar. Except for a few point sources, the emission rates of ozone precursors are low in the remote regions surrounding the

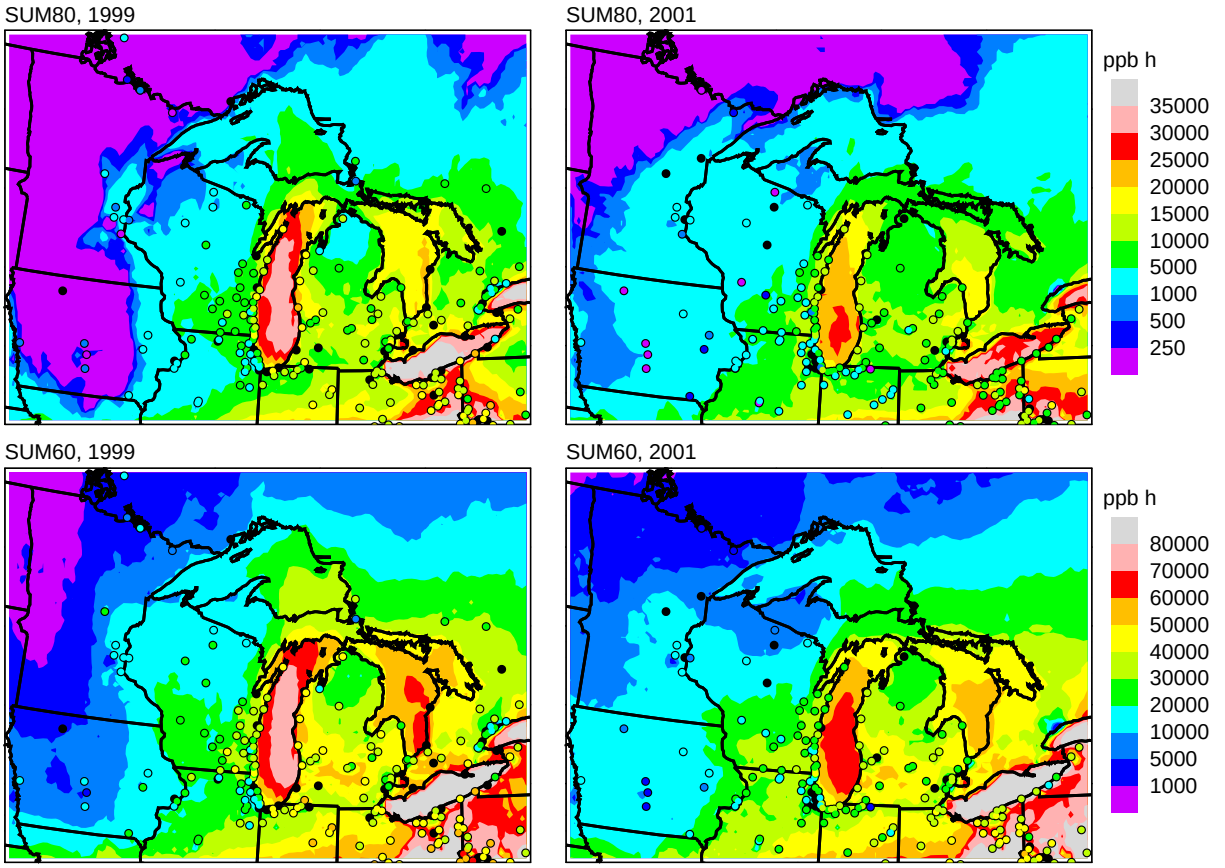

Fig. 8. Observed (dots) and predicted (contours) seasonal ozone exposure for 1999 and 2001. Black dots denote missing data.

Great Lakes in the northern third of the domain. The ozone exposure in these areas was produced primarily by northerly transport of ozone. The simulated ozone exposure distributions that extended into the upper peninsula of Michigan and Ontario indicate that northerly transport of ozone occurred frequently.

The model also produced lower SUM80 values over and near the Great Lakes during 2001 than during 1999, consistent with the observations. There are parts of the domain, however, where higher concentrations were predicted in 2001 (e.g. Minnesota, Iowa, and northern Michigan). While the simulated SUM60 during 2001 was somewhat lower than during 1999, the magnitude was still higher than observed in the southern portion of the domain. The overall pattern of the simulated ozone exposure between the two years was similar, except that the predicted ozone mixing ratios in the northern Great Lakes region suggest that the meteorological conditions during the summer of 2001 were less favorable for the northerly transport of ozone than during 1999.

A quantitative evaluation of the monthly observed and simulated ozone exposure is shown in Fig. 9. The simulated mean ozone exposure at the ozone monitoring stations was similar to the observed value for most months, except for August 2001. During that month, the predicted mean and range ozone exposure was significantly higher than observed. Nevertheless, the figure suggests that the model also reproduced the monthly variations in ozone exposure in addition to the seasonal exposure distributions shown in Fig. 8.

4.4. Effect of future anthropogenic emissions

Since the model was able to reproduce the overall meteorological conditions and ozone distributions during the two summer periods, we also used the model to investigate the effect of projected emission rate scenarios (IPCC SRES B2 marker scenario (IPCC, 2000)) appropriate for years 2020 (emission scenario 'A') and 2040 (emission scenario 'B') on the overall ozone exposure when the same 1999 and 2001 meteorology is applied.

The resulting differences in seasonal SUM60 and SUM80 between the emission scenario 'A' and 'B' and control simulations are shown in Figs. 10 and 11,

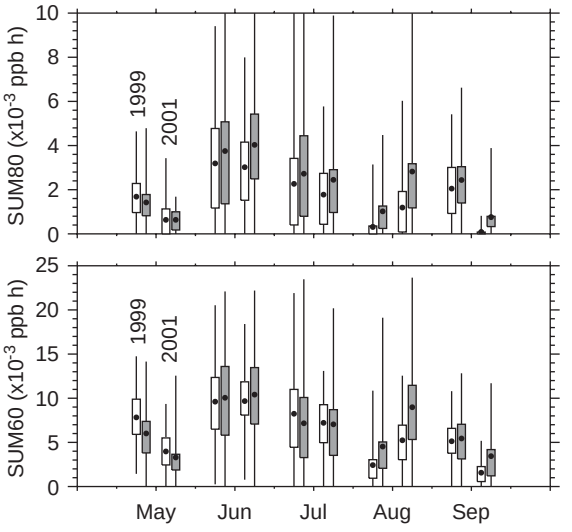

Fig. 9. Observed (black) and simulated (gray) SUM60 and SUM80 over the Great Lakes region during the summer of 1999 and 2001. The vertical lines denote the range, the boxes denote the 25% and 75% quantiles, and the dots the average among the monitoring stations shown in Fig. 1.

respectively. The overall patterns associated with emission scenarios 'A' and 'B' are similar, but the difference plots indicate that the magnitude of the ozone exposure was higher in emission scenario 'B'. For the simulation that employed the meteorological conditions during 1999, the changes in anthropogenic emissions increased nitrogen oxide titration, that in turn, reduced ozone levels in the immediate vicinity the large metropolitan areas of Chicago, Milwaukee, Detroit, and Cleveland. Higher levels of nitrogen oxide emissions, however, also increased ozone production downwind of the emission sources. The increased frequency and duration of high ozone episodes that were transported to the north and east had the largest effect on ozone exposure levels over remote, less populated regions. A significant increase in SUM80 was predicted over most of Michigan and downwind over the northern Great Lakes region. The changes in the SUM60 distribution were similar, except that there were increases in ozone exposure over the largely rural agricultural regions of Minnesota, Wisconsin, Illinois, and Indiana.

In contrast to 1999, a modest increase in ozone exposure was predicted in isolated areas by the

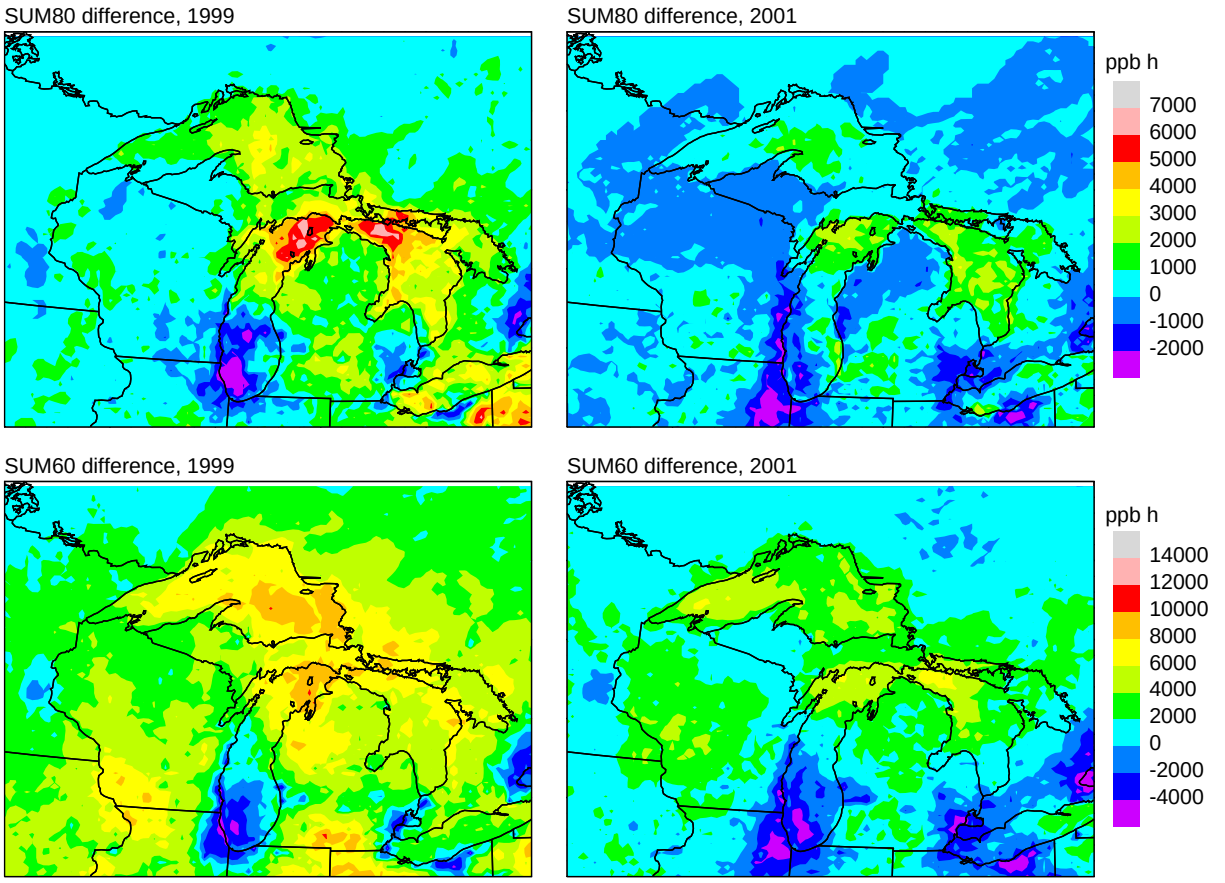

Fig. 10. Difference in predicted ozone exposure (emission scenario 'A' simulations—control simulations) for 1999 and 2001.

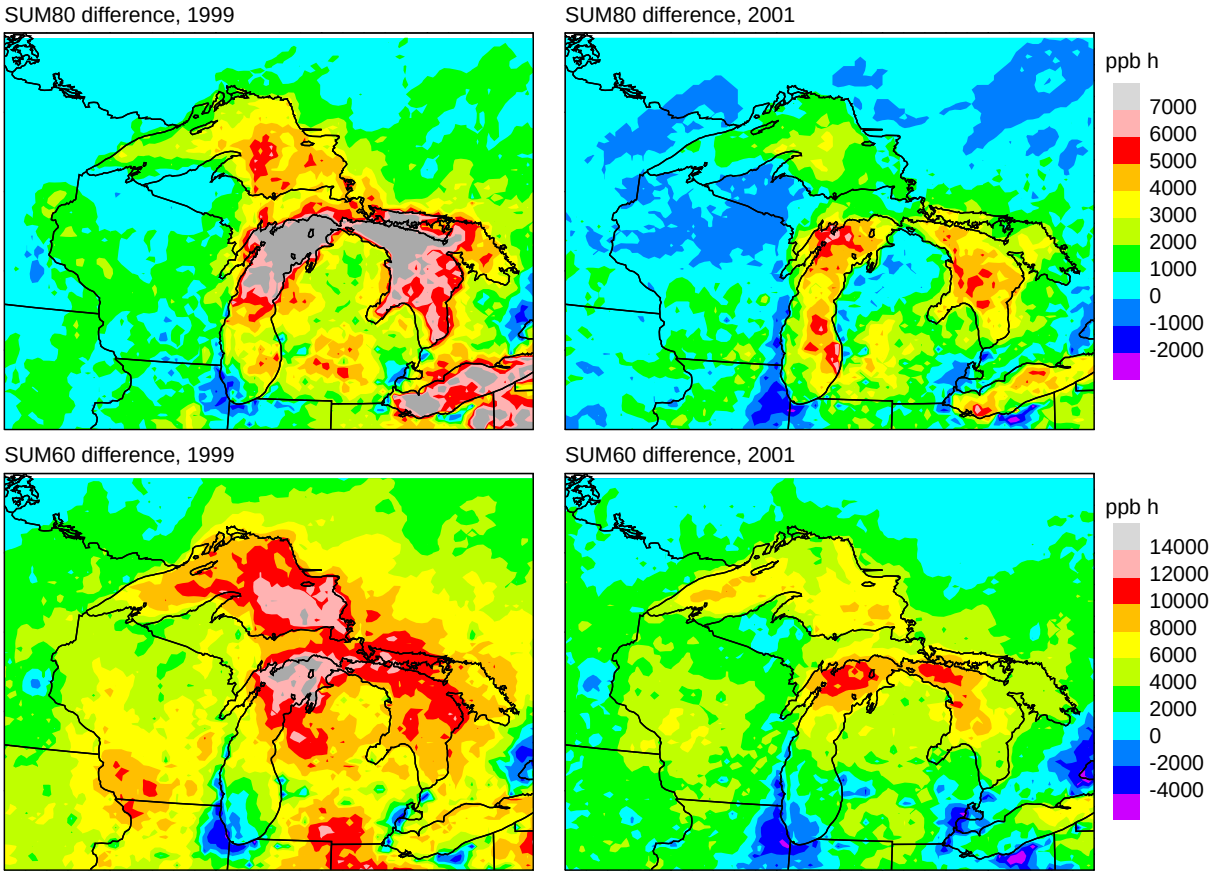

Fig. 11. Same as Fig. 10, except for emission scenario 'B' simulations.

simulation employing the 2001 meteorological conditions that were less favorable for ozone production. Most of the increases in ozone exposure were produced only over the lake surfaces. These results suggest that changes in future air quality will depend significantly on the meteorological conditions and predictions of future air quality will require an understanding of how climate change can affect average synoptic conditions in the region.

As demonstrated in Tao et al, (2003), some of the changes in ozone exposure shown in Figs. 11 and 12 are likely due to synergistic contributions between anthropogenic emissions and biogenic emissions. This contribution, however, is not quantified in this study.

The spatial variations in ozone exposure were quantified for six forested regions surrounding the northern Great Lakes as shown in Fig. 12. Ozone precursor emissions in these regions were usually much smaller than in other portions of the domain, except for several point sources, so ozone mixing ratios greater than 80 ppb resulted primarily from transport. The SUM80 ozone exposure was usually small for both 1999 and 2001 in regions 1, 2, and 3 because of the infrequent occurrence of high ozone concentrations transported into the region. During periods of southerly or southeasterly synoptic winds that were favorable for transport into regions 1, 2, and 3, dilution and chemical destruction processes decreased ozone mixing ratios to less than 80 ppb as the pollutant plumes were transported northward. The meteorological conditions during both 1999 and 2001 that produced frequent southwesterly flow often transported ozone mixing ratios exceeding 80 ppb into regions 4, 5, and 6. As indicated by the low SUM80 values, transport of high ozone concentrations did not occur every month. The monthly variations of SUM60 were similar to those for SUM80, and the values for regions 4, 5, and 6 were significantly higher than for regions 1, 2, and 3. Ozone mixing ratios occasionally exceeded 60 ppb around Lake Superior during a number of months for both 1999 and 2001.

The monthly differences in SUM80 and SUM60 between the control and emission scenario 'B' simulations are shown in Fig. 12 as well. The higher anthropogenic emission rates produced a small increase in ozone exposure for the meteorological conditions of

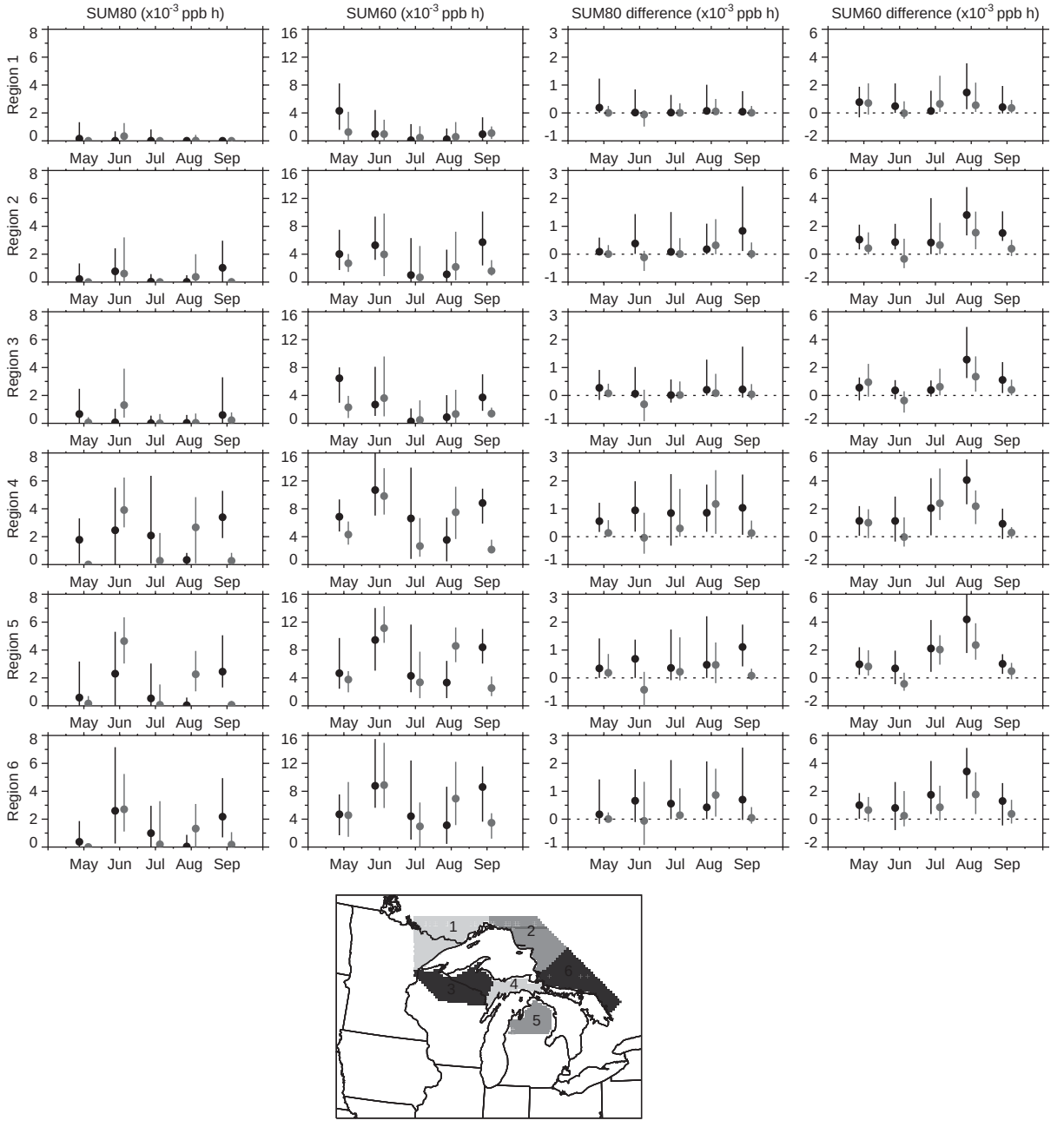

Fig. 12. Mean and range of SUM80 and SUM60 over 6 regions surrounding the Great Lakes for the control simulations. Differences in SUM80 and SUM60 between the emission simulations 'B' and the control simulations given in the right two panels. Black and gray denote values using the 1999 and 2001 meteorological conditions, respectively.

1999 at a few grid cells within regions 1, 2, and 3, but the average ozone exposure averaged over the region was nearly the same for the two simulations. However, within regions 4, 5 and 6 monthly SUM80 during 1999 increased by as much as 2000 ppb h. Average monthly ozone exposure from the emission scenario simulation usually was 25–50% higher than the control simulation, although larger increases occurred at specific grid cells and for months in which the exposure was close to zero in the control simulation. For the meteorological conditions during 2001, SUM80 from the control and emission scenario simulations were usually the same for

regions 1, 2, and 3 and small increases in SUM80 were predicted only during a few months for regions 4, 5, and 6. Monthly SUM60 from the emission scenario simulation was higher than the control simulation for nearly every month of 1999 and 2001. Increases in SUM60 varied more month by month than did the increases of SUM80. The largest increase in SUM60 occurred for August of 1999 in which average ozone exposure over regions 4, 5, and 6 doubled. As with SUM80, the increases in SUM60 occurred only during a few months for the meteorological conditions during 2001.

5. Summary

A coupled meteorological and chemical modeling system was used to simulate the evolution of ozone over the Great Lakes region between May and September of 1999 and 2001. The summer of 1999 was favorable for ozone production, while the summer of 2001 was less favorable because of increased frequency of northwesterly winds that transported ozone and ozone precursors out of the region. The overall temporal and spatial variations in hourly ozone concentrations and ozone exposure from the control simulation agreed reasonably well with the observations at most locations for both summers. The average bias, RMSD, and IA was −0.5 (1.5), 19.4 (20.1), and 0.74 (0.69) for the summer of 1999 (2001), respectively. The simulated ozone exposure was higher during the summer of 1999 than during 2001, similar to the observations, indicating that the model could be used to examine the sensitivity of ozone predictions to anthropogenic trace gas emission rates. Additional simulations were performed that increased anthropogenic emissions of NOx and VOCs based on the IPCC SRES B2 scenarios for the years 2020 and 2040. In emission scenario 'A', NOx and VOCs were increased by a factor of 1.25 and 1.08, respectively, while for emission scenario 'B' they were increased by a factor of 1.35 and 1.25, respectively.

The emission scenario simulations applied to the 1999 meteorology produced increases in ozone exceeding 80 ppb over the lower peninsula of Michigan, the eastern half of the upper peninsula of Michigan, and over Ontario just north of Lake Superior and Lake Huron. Despite the increase in anthropogenic emissions, increases in SUM80 only occurred over the lake surfaces and in central Michigan when the 2001 meteorology was applied. For both meteorological scenarios, increases in anthropogenic emissions decreased ozone exposure in the immediate vicinity of the largest metropolitan areas, such as Milwaukee, Chicago, Detroit, and Cleveland, as a result of NO titration. While the spatial distribution of the increases in SUM60 for the 1999 meteorology was similar to those of SUM80, relatively large increases also were produced over agricultural regions in the southern half of the model domain. As with SUM80, the increases in SUM60 for the 2001 meteorology were relatively small.

The simulated ozone from this study will be used in the near future as input to biological models to assess the potential response of ozone-sensitive tree species to current and future ozone levels in the Great Lakes region. An important factor in predicting future air quality is the magnitude and spatial distribution of projected emission rates. Projections of anthropogenic emissions rates of ozone precursors are highly uncertain because they depend on assumptions of population, economic development, land-use patterns, and technology. Therefore, the effect of increased anthropogenic emission rates on ozone levels and the spatial distribution of ozone in the Great Lakes region could be much larger or smaller than indicated by this study.

Research on the complex linkages between changes in climate, increases in anthropogenic emissions, landscape change, and regional air quality has just begun. This study demonstrates that for certain meteorological situations, ozone levels outside of urban areas remain the same or decrease despite significantly higher anthropogenic emission rates. Higher ozone levels outside of urban areas occurred for meteorological conditions that were already favorable for ozone production, such as high-pressure systems with clear skies, warm temperatures, and northerly transport. Therefore, ozone levels that impact human and vegetation health in the Great Lakes region will depend on the interaction of changes in anthropogenic emissions, and the frequency and persistence of high-pressure systems predicted by climate models. The results of this study also demonstrate that the predicted effectiveness of emission control strategies will be dependent on the meteorological conditions used for modeling the impact of such strategies.

Acknowledgements

This research was supported by the USDA Forest Service under Interagency Agreement # 02-IA-11231300-047. This research was performed in part using the Molecular Science Computing Facility (MSCF) in The William R. Wiley Environmental Molecular Sciences Laboratory, a national scientific user facility sponsored by The U.S DOE and located at PNNL. The Pacific Northwest National Laboratory is operated for the DOE by Battelle Memorial Institute under contract DE-AC06-766RLO 1830. We thank Timothy Trapp (Wisconsin Department of Natural Resources) for providing the Badger ferry ozone data and Mary Anne Carroll (University of Michigan) for providing the PROPHET ozone data. Ozone data were provided by the US EPA and the Environment Canada's

NAPS network. We greatly appreciate the comments from two anonymous reviewers that improved this manuscript.

References

Brasseur, G.P., Kiehl, J.T., Muller, J.-F., Schenider, T., Granier, C., Tie, X.X., Hauglustaine, D., 1998. Past and future changes in global tropospheric ozone: impact on radiative forcing. Geophysics Research Letters 25, 3807–3810.

Civerolo, K.L., Sistla, G., Rao, S.T., Nowak, D.J., 2000. The effects of land use in meteorological modeling: implications for assessment of future air quality scenarios. Atmospheric Environment 34, 1615–1621.

Constable, J.V.H., Guenther, A.B., Schimel, D.S., Monson, R.K., 1999. Modeling changes in VOC emissions in response to climate change in the continental United States. Global Change Biology 5, 791–806.

Danielsen, E.F., Hipskind, R.S., Gaines, S.E., Saches, G.W., Gregory, G.L., Hill, G.F., 1987. Three-dimensional analysis of potential vorticity associated with tropopause folds and observed variations of ozone and carbon dioxide. Journal of Geophysics Research 92, 2103–2111.

Fast, J.D., 1995. Mesoscale modeling in areas of highly complex terrain employing a four-dimensional data assimilation technique. Journal of Applied Meteorology 34, 2761–2782.

Fast, J.D., Heilman, W.E., 2003. The effect of lake temperatures and emissions on ozone exposure in the western Great Lakes region. Journal of Applied Meteorology 42, 1197–1217.

Fast, J.D., Zaveri, R.A., Bian, X., Chapman, E.G., Easter, R.C., 2002. The effect of regional-scale transport on oxidants in the vicinity of Philadelphia during the 1999 NE-OPS field campaign. Journal of Geophysics Research 107, 10.1029/2001JD000980.

Fiore, A.M., Jacob, D.J., Field, B.D., Streets, D.G., Fernandes, S.D., Jang, C., 2002. Linking ozone pollution and climate change: the case for controlling methane. Geophysics Research Letters 29, 10.1029/2002GL015601.

Guenther, A.B., Zimmerman, P.R., Harley, P.C., Monson, R.K., Fall, R., 1993. Isoprene and monoterpene emission rate variability: model evaluation and sensitivity analyses. Journal of Geophysics Research 98, 12,609–12,617.

Helfand, H.M., Labraga, J.C., 1988. Design of a nonsingular level 2.5 second-order closure model of the prediction of atmospheric turbulence. Journal of Atmospheric Science 45, 113–132.

Hogrefe, C., Lynn, B., Civerolo, K., Ku, J.-Y., Rosenthal, J., Rosenzweig, C., Goldberg, R., Gaffin, S., Knowlton, K., Kinney, P.L., 2004. Simulating changed in regional air pollution over the eastern United States due to changed in global and regional climate and emissions. Journal of Geophysics Research, 109.

Hogsett, W.E., Weber, J.E., Tingey, D., Herstrom, A., Lee, E.H., Laurence, J.A., 1997. Environmental auditing: an approach for characterizing tropospheric ozone risk to forests. Environment Management 21, 105–120.

Houyoux, M.R., Vukovich, J.M., Coats Jr., C.J., Wheeler, N.W., Kasibhatla, P.S., 2000. Emission inventory development and processing for the seasonal model for regional air quality (SMRAQ) project. Journal of Geophysics Research 105, 9079–9090.

Intergovernmental Panel on Climate Change, 2000. Special report on emissions scenarios. In: Nacenovic, N., Swart, R. (Eds.). Cambridge University Press, New York, p. 612.

Intergovernmental Panel on Climate Change, 2001. Climate change 2001: The scientific basis. In: Houghton, J.T., et al. (Eds.). Cambridge University Press, New York, p. 944.

Jacob, D.J., Logan, J.A., Murti, P.P., 1999. Effect of rising Asian emission on surface ozone in the United States. Geophysics Research Letters 26, 2175–2178.

Johnson, C.E., Collins, W.J., Stevenson, D.S., Derwent, R.G., 1999. Relative roles of climate and emission changes on future tropospheric oxidant concentrations. Journal of Geophysics Research 104, 18,631–18,645.

McKee, D.J. (Ed.), 1994. Tropospheric ozone: Human health and agricultural impacts. Lewis Publishers, p. 333.

Mellor, G.L., Yamada, T., 1982. Development of a turbulence closure model for geophysical fluid problems. Reviews in Geophysics and Space Physics 20, 851–875.

Olivier, J.G.J., Berdowski, J.J.M., 2001. Global emission sources and sinks. In: Berdowski, J., Guicherit, R., Heij, B.J. (Eds.), The Climate System. A.A. Balkema Publishers/Swets & Zeitlinger Publishers, Lisse, The Netherlands, pp. 33–78.

Prather, M., Gauss, M., Bernsten, T., Isaksen, I., Sundet, J., Bey, I., Brasseur, G., Dentener, F., Derwent, R., Stevenson, D., Grenfell, L., Hauglustaine, D., Horowitz, L., Jacob, D., Mickley, L., Lawrence, M., von Kuhlmann, R., Muller, J.-F., Pitari, G., Rogers, H., Johnson, M., Pyle, J., Law, K., van Weele, M., Wild, O., 2003. Fresh air for the 21st century? Geophysics Research Letters, 30.

Schwab, D.J., Leshkevish, G.A., Muhr, G.C., 1992. Satellite measurements of surface water temperature in the Great Lakes—Great Lakes coastwatch. Journal of Great Lakes Research 18, 247–258.

Tao, Z., Larson, S.M., Wuebbles, D.J., Williams, A., Caughey, M., 2003. A summer simulation of biogenic contributions to ground-level ozone over the continental United States. Journal of Geophysics Research, 108.

US EPA, 2004. 1970–2002 Average annual emissions. All criteria pollutants. US Environmental Protection Agency, Washington DC, available http:\\www.epa.gov/ttn/chief/trends/tends02/trendsreportallpollutants111504.xls.

Vukovich, F.M., 1987. A note on air quality in high pressure systems. Atmosheric Environment 13, 255–265.

Vukovich, F.M., 1995. Regional-scale boundary layer ozone variation in the eastern United States and their association with meteorological variations. Atmosheric Environment, 2259–2273.

Willmott, C.J., 1982. Some comments on the evaluation of model performance. Bulletin of the American Meteorological Society 63, 1309–1313.

Yienger, J.J., Galanter, M., Holloway, T.A., Phadis, M.H., Guttikunda, S.K., Carmichael, G.R., Moxim, W.J., Levy II, H., 2000. The episodic nature of air pollution transport from Asia to North America. Journal of Geophysics Research 105, 26,931–26,946.